

# HIGH ACCURACY HANDHELD MAPPING SYSTEM FOR FAST HELICOPTER DEPLOYMENT

J. Skaloud<sup>a,\*</sup>, J. Vallet<sup>b</sup>

<sup>a</sup> Geodetic Engineering Laboratory,

<sup>b</sup> Laboratory of Photogrammetry,

Swiss Federal Institute of Technology (EPFL), 7, Avenue Piccard, CH - 1015 Lausanne, Switzerland

[jan.skaloud@epfl.ch](mailto:jan.skaloud@epfl.ch), [julien.vallet@epfl.ch](mailto:julien.vallet@epfl.ch)

Commission IV, WG IV/7

**KEY WORDS:** Aerial, Mobile, Disaster, Mapping, GPS, Precision, Sensor, Fusion.

## ABSTRACT:

This paper presents a self-contained, light and flexible mapping system that can be quickly deployed into inaccessible areas. Although designed to measure wind-transported snow volumes and the snow avalanche runoff over an experimental site, the system is suitable to any large-scale 3-D terrain mapping. The system comprises of a supporting electronic that is loosely linked to a light but ridged sensor block containing a camera, an IMU and a GPS antenna. The relatively small size and weight of the sensor block permits manual pointing of the camera (film-based or digital) towards either the mountain face or the valley bottom. Such hand-held steering allows mapping of the avalanche release and deposit zones during the same flight and also dampens the engine-induced vibration. The exterior orientation (EO) parameters of the camera are determined directly by GPS/IMU integration. The orientation performance of the navigation solution is improved by integrating the data from a second GPS antenna placed on the helicopter tail. Once the system is calibrated and with EO determined the mapping procedure implies only the forward resection without the need of aerial triangulation (AT) and ground control points. The practical experiences have demonstrated a mapping accuracy of 10cm and 15cm in the horizontal and vertical, respectively.

## RÉSUMÉ:

Cet article présente un système de cartographie indépendant, léger et flexible qui peut être rapidement utilisé dans des zones inaccessibles. Bien que conçu à l'origine pour mesurer des volumes de neige transportés par le vent ou par des avalanches sur un site expérimental, le système convient également à toute cartographie 3D à grande échelle du terrain. Le système comporte une structure rigide et légère, supportant une caméra, une unité inertielle et une antenne GPS, qui est liée à l'électronique d'acquisition et de traitement. Le faible poids et l'encombrement restreint de la structure permet d'orienter manuellement la caméra (analogue ou digitale) de manière oblique ou verticale. Ce maintien manuel du système permet de saisir la zone de dépôt et la zone de déclenchement de l'avalanche lors du même vol et d'amortir les vibrations induites par l'hélicoptère. Les paramètres de l'orientation externe (EO) de la caméra sont directement déterminés par l'intégration IMU/GPS. La précision d'orientation de la solution de navigation est améliorée par l'intégration d'une seconde antenne GPS sur la queue de l'hélicoptère.

Une fois le système calibré et l'orientation externe déterminée, la procédure de cartographie nécessite uniquement une résection inverse sans avoir recours à une aérotriangulation (AT) avec des points d'ajustage au sol. Des tests pratiques est ressortie une précision de 10cm en planimétrie et 15cm en altimétrie sur la mesure de points au sol.

## 1. INTRODUCTION

### 1.3 Motivation

The sporadic and erratic occurrence of avalanches or landslides requires mapping systems that are flexible and can be quickly deployed into inaccessible areas. Furthermore, periodic mapping of avalanche test sites or natural hazard areas is sometimes required as in the particular case of Alps (Issler, 1999). The relatively small size of these areas, their spatial characteristics and their seasonal use put particular prerequisites on the mapping system:

### 1.4 System Requirements

- fast set-up and availability (days or hours)
- relative independence from a particular carrier

- possibility to map near vertical (mountain faces) and horizontal (valley bottoms) features during the same flight
- high relative and absolute mapping accuracy (~20cm)
- no assistance of ground control points.

### 1.5 Choice of a System Concept

Considering the above mentioned requirements, two appropriate concepts can be considered:

- large scale photogrammetry using handheld light aerial camera coupled with a GPS/INS sensors
- laser scanner (i.e. LIDAR) integrated with a GPS/INS.

The differences between these two concepts are highlighted in the Table 1 bellow.

Handheld Camera, GPS/INS	LIDAR, GPS/INS
	accuracy - see Section 5
+ fast set-up time (<20 min)	- long set-up time
+ independent from a carrier	- particular requirements
- contrast dependent	+ illumination independent
+ mountain faces mapping	- steep slopes mapp. limited
- semi-automatic mapping	+ automatic DTM generation
+ direct cost: \$100K	- direct cost: \$1500K
+ low cost for small areas	- high cost for small areas

Table 1. Comparison between different mapping approaches.

The use of an airborne laser scanning system may be appealing mainly due its automatic generation of DTM and its independence of surface illumination. However, its acquisition cost cannot usually be justified by the small application scale and its seasonal use. Moreover, the portability of the laser scanning system between different carriers is limited because of specific demands (e.g., floor view) and the long set-up time. The cost of having a designated system carrier is therefore another prohibiting factor for such type of application. An alternative solution by mandating a third-party service provider is not suitable due to the need of system availability on a short-time notice. To conclude this discussion, although both concepts are most likely comparable in terms of accuracy, the photogrammetric approach was chosen as the better suited due to its improved flexibility, higher versatility, lower acquisition costs and relative independence from a particular rescue helicopter.

The choice of a helicopter as the mapping system carrier is justified by its capability to fly close to the ground at low speed. This allows capturing photographs in large-scale and provides better flight line navigation. In following, particularities of the system will be described together with an analysis of its performance.

## 2. AIRBORNE DATA COLLECTION SYSTEM

The system can be divided into three essential parts:

- light and rigid sensor block (Figure 1), comprising of a handheld aerial camera (film or digital), GPS antenna and an IMU
- a second GPS antenna placed on the tail of the helicopter
- the supporting electronic, i.e. the GPS receivers, GPS/INS integrator and data logger (Figure 2)

### 2.1 Imagery Component

Two film-based aerial cameras have been successfully tested, while implementation of a digital one is on the way. The system prototype used a light handheld Linhof Aerotechnika camera that stores up to 200 colour, large format photographs (4x5 inches) and has a 90mm wide angle lens. Its total weight reaches 8kg. The most recent testing have been conducted with the Tomtecs HIEI G4 with 370 colour pictures capacity, 5x5 inch format and 90mm lens. Both cameras fulfil the required flexibility and provides images of high quality. While the Tomtecs camera offers an internal synchronisation with the GPS time, the employment of Linhof camera required additional installation of photodiodes and a RC circuit that sense the shutter open and sends an event-input pulse towards the data logger.

### 2.2 Navigation Component

The system currently employs two Leica SR530 GPS receivers on the helicopter and additional GPS receiver/s on the ground. The IMU is a customised tactical-grade strapdown inertial system (LN-200) with fibre-optic gyros. A real-time GPS/IMU integrating component was provided by Dynamic Research Corporation (DRC, 2001). It integrates the IMU data with the Trimble Force 5 military receiver over the VME (Versa Module Eurocard) bus in real-time and at 400Hz. The navigation solution is stored concurrently with the IMU data. When high orientation accuracy is required the recorded IMU data are used in a post-mission integration with the differential carrier phase GPS data.

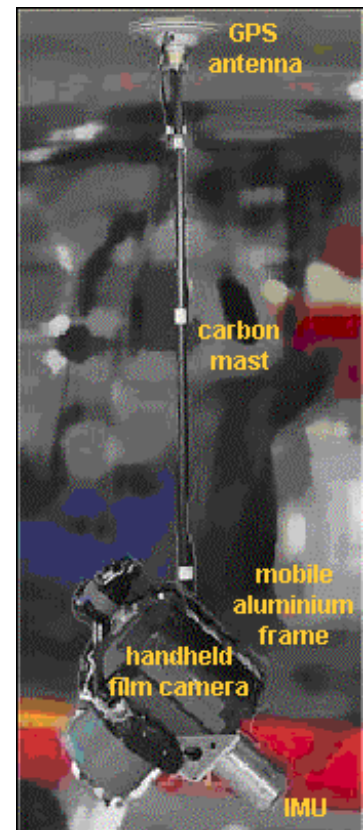


Figure 1. The sensor block.



Figure 2. The sensor supporting electronic that is quickly installable.

### 2.3 Helicopter Mount

The placement of the sensors in the helicopter was chosen to comply with the following requirements:

- prevent any differential movements between sensors
- reduce the disturbing effect of the vibrations

- enable manual orientation of the camera to capture oblique as well as vertical imagery
- offer a firm attachment of the sensor block that can facilitate long transition flights and can permit the use of a GPS-derived azimuth during the period of IMU-alignment

Addressing the first objective, a light and rigid steel-aluminium-carbon holder was designed to connect all sensors within a rigid block as shown in Figure 1. Its relatively small size permits handholding. This responds to the other two requirements as the vibrations are dampened through the body of an operator (Figure 3) who can also aim the camera to a desirable direction. The last requirement is fulfilled by a steel socket-joint by which the system can be quickly attached to the side of a helicopter.

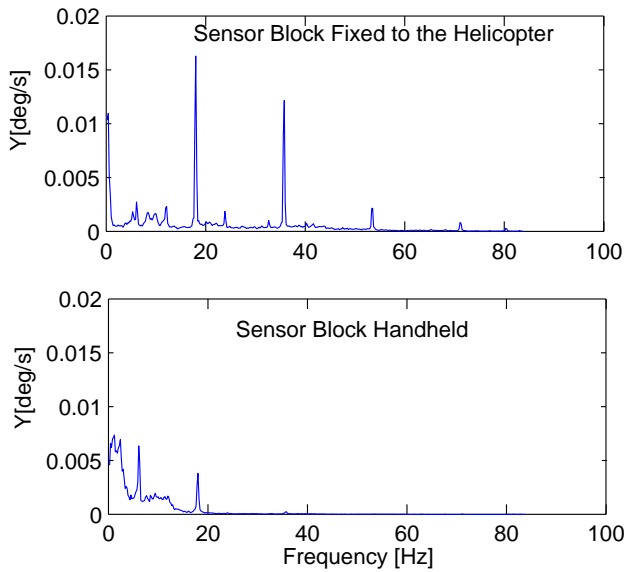


Figure 3. Amplitude spectrums of y-gyro signal computed during the transition flight and the picture session.

## 2.4 Operational Procedure

At the transition period of a flight the system is stiffly mounted outside the helicopter on a steel frame. During this time, the data from a second GPS antenna provide the supplementary azimuth important for achieving the precise alignment of the inertial system. At the beginning of the picture session, the camera-IMU-GPS block is removed from its holder through the side door to handhold by the operator. This allows manual orientation towards the mountain face around the omega angle. The sensor block can be fixed again during another flight transition period, or in a long flight line.

## 3. NAVIGATION DATA PROCESSING

Simulations and practical experience have shown that camera EO parameters need to be determined with an accuracy of 5-15cm in position and 0.005-0.008deg in orientation to satisfy the highest requirements of 10-30cm on the mapping accuracy (Vallet et al., 2000).

As the real-time GPS/INS navigation solution is accurate to 10-20m in position and  $\sim 0.1$ deg in orientation, following data processing scheme is adopted either entirely, or partially to rise

up the EO estimate to an appropriate level according to the mapping requirements.

### 3.1 Carrier Phase Differential GPS (CPDGPS)

The processing of the GPS code and carrier phase data is the determining factor of positioning accuracy. Depending on the number and the distribution of the base stations, the superior accuracy limit is most likely 5-10cm in the position. *GrafNav/GrafMov* (Waypoint Consulting Inc., 2001) processing engine is used for that purpose and a search is on the way to supply the user with an automated and reliable data handling. As the measurement frequency of the employed GPS receivers is 10Hz, the trajectory is sufficiently over-sampled to accurately interpolate the events of camera exposure.

### 3.2 Post-Mission GPS/INS Filtering and Smoothing

The approximate orientation accuracy at real-time is at 0.1deg. When higher accuracy is required, the recorded inertial measurements need to be integrated with the position and velocity data based on the CPDGPS estimate computed in the previous step. The *POSProc* (Applanix Corp., 2000) represents a fine tool for such a purpose as it optimally blends the inertial data with different kinds of navigation data via centralised Kalman filtering/smoothing configuration. The versions prior to 3.0 are furthermore ideal for a developer, as they permit to fine-tune the Kalman filter parameters to specific scenarios and IMUs. Automated data treatment and evaluation can also be achieved by the batch processing and is planned to be implemented in future.

### 3.3 GPS-Azimuth Aiding

It is a well-known fact that updating an inertial system with navigation information of better quality prevents the unbounded growth of position and attitude errors. As usually, GPS provides a mean of 'in-flight alignment' of the inertial system, removing the need for performing the 'north seeking' process prior to the flight. However, the accuracy of the in-flight alignment is strongly affected by the dynamic of the carrier. Since the accelerations induced by helicopter manoeuvres are

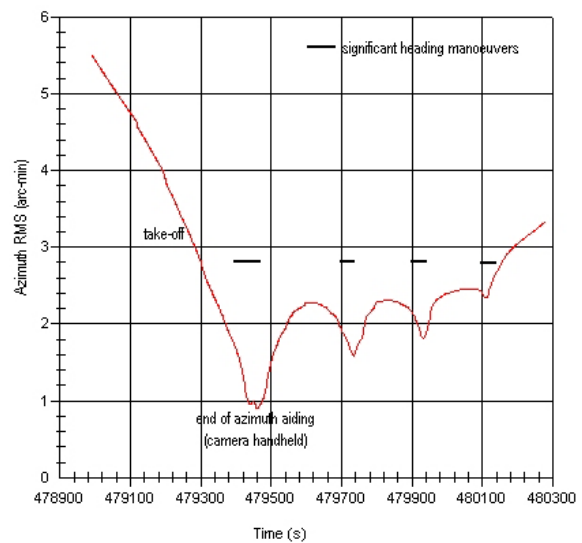


Figure 4. The effect of aircraft manoeuvres and GPS-derived azimuth aiding on the estimated azimuth accuracy.

considerably smaller than those of an aircraft, this problem needs to be circumvented by other means.

Here, the necessary information is derived from a second GPS antenna placed at the tail of the helicopter. Thanks to a relatively long (5 meter) separation between the two GPS antennas, the derived azimuth is sufficiently accurate and can be used as an additional information aiding the IMU. Again, the *GrafNav/GrafMov* software package is employed for calculating the relative vector between the two moving GPS antennas.

The theoretical effect of GPS-azimuth aiding on the INS alignment is depicted in Figure 4, while the practical experience showed that this helps in achieving alignment accuracy of better than 0.01deg in the azimuth. Furthermore, this accuracy can be maintained even during long flight lines but requires the camera to remain fixed in its holder.

#### 4. SYSTEM CALIBRATION

The calibration of the sensors involves determining the relative displacement and orientation differences (boresight) between the camera and the inertial system, the parameters of the interior orientation as well as the constant synchronisation offsets inherently present due to data transmission and internal hardware delays.

##### 4.1 Camera Calibration

The calibration of the camera consisted of two phases. First, the focal length, the principal point and the radial distortion were calibrated during a preliminary flight over a well signalled test field using the GPS-assisted AT. They were primary introduced together as unknowns into the *Bingo-F* bundle adjustment software (Kruck, 2001), while their final estimate was performed separately by iterations.

A second calibration phase was performed when large residual systematic effects were observed under extremely cold winter conditions. Investigation revealed a significant shift of the camera projection centre, 200um and 50um, respectively, and also detected defaults in the flatness of the vacuum plate in the

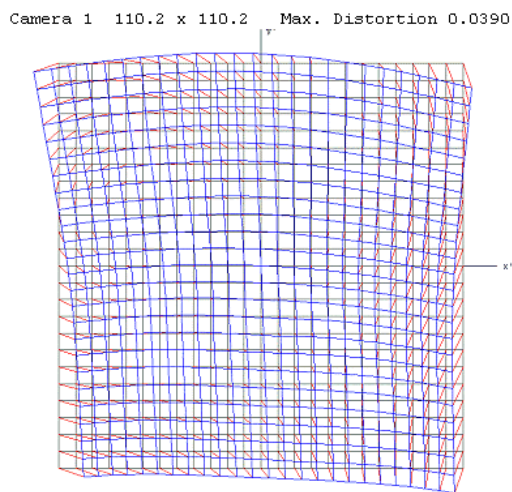


Figure 5. Non-radial deformations due to the flatness defaults of the vacuum plate.

range of -45um to +17 um. The latter was compensated by introducing additional non-radial deformation parameters as depicted in Figure 5.

##### 4.2 Sensor Placement

The relative displacements among the individual components of the sensor block were measured terrestrially in the image frame and with sub-centimetre precision. A good knowledge of these parameters subsequently produces better boresight calibration and also allows reducing the size of a Kalman filter for the lever-arm components in GPS/INS integration.

##### 4.3 Boresight Calibration

The determination of the relative orientation displacement between the camera's image frame and the IMU's body frame requires the use of a well-designed block of images of a strong geometry. As the usual implementation of the AT concept results in a strong correlation between the parameters of exterior orientation, the introduction of GPS/INS observations for the camera perspective centre positions into the bundle adjustment is recommended (Skaloud, 2002). Such approach also permits the concurrent calibration of the parameters of interior orientation (Schmitz et al., 2001).

The evolution of the estimated boresight angles is depicted in Figure 6. This method also provides good indication of the relative orientation accuracy of the navigation system when the AT-estimated orientation is significantly more precise. The 1- $\sigma$  values of ~0.01deg are certainly fulfilling the demanding expectations.

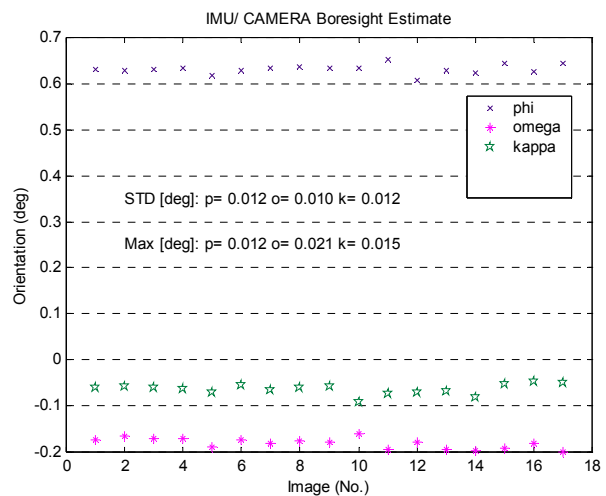


Figure 6. The evolution of the boresight parameters.

#### 5. PRACTICAL EXPERIENCES

The results of snow surface restitution by photogrammetric means were reported previously (Vallet et al., 2000). The following evaluation will therefore focus on the system absolute accuracy at discrete points. A test field of about 25 Ground Control Points (GCP's) will serve for this purpose.

The scale of the images that were taken over this test field varies between 1:3000-1:4000 and the accuracy of ground control points is at 2cm level. Some GCP's are not specially signalled and therefore the measurement of their image coordinates may introduce additional error between 7-20um (i.e. 3-8cm in the object space).

### 5.1 Residuals in Object Space

Figure 7. depicts the 3D residuals on all ground control points when neither GCP nor tie-points are used. In other words, the EO parameters for each image are used as supplied by the navigation system and only forward intersection is carried out. It can be concluded from the plot that about 95% of the residuals lies between the  $\pm 0.15\text{cm}$  and  $\pm 25\text{cm}$  in the horizontal and vertical components respectively. The size of the residuals depends partially on the number of intersections implemented and will be further analysed.

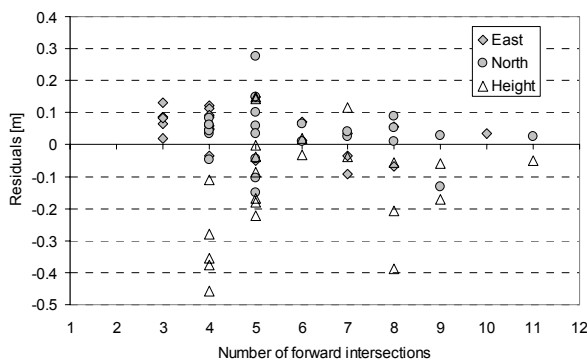


Figure 7. Residuals on control points obtained by forward intersections, i.e. direct georeferencing without the use of tie points and ground control.

### 5.2 Accuracy in Object Space

To better estimate the performance of the system, additional 300 points were determined by the AT concept within a block of photographs. Due to the high measurement redundancy, the accuracy of these points is estimated to be 5-10cm. Subsequently, the coordinates of these points were compared to those obtained by forward resection, i.e. by direct georeferencing. The points were grouped into the classes according to the number of intersections and the RMS values were calculated from the observed differences (Figure 8).

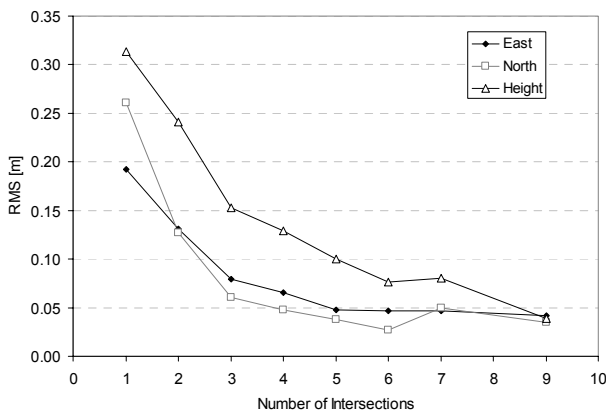


Figure 8. Direct georeferencing accuracy as a function of number of intersections.

As can be seen from this plot, the accuracy improves by a factor of two when moving from the minimum of 1 to 3 intersections (i.e. from 30cm to 15cm). It is also interesting to observe that the higher number of intersections does not longer improve the horizontal accuracy, as the precision of our reference is reached. This takes slightly longer for the vertical component that is influenced by the weaker geometry of the intersecting arrays.

### 5.3 Comparison to AT

The indirect (AT, AT/GPS) and direct (GPS/INS) approaches to photogrammetric mapping are compared in Table 1 in terms of empirically estimated accuracy. Although, the RMS values for the direct method are slightly bigger they still comply with the demand on the system to deliver  $\leq 20\text{cm}$  mapping accuracy. Adopting the direct approach, however, avoids the difficulties encountered in performing the automated AT in mountainous areas. This considerably increases the operational flexibility for natural disaster mapping.

Method	Constrains		RMS at GCP's [cm]		
	GCP	Block	East	North	Height
AT	•	•	5	4	4
AT/GPS		•	6	6	8
Direct			8	9	20

Table 2. Comparison of empirically obtained mapping accuracy for different approaches to EO determination as well as their operational constrains.

### 5.4 Comparison to a Laser Scanning System

The mapping accuracy of the proposed method is practically independent from the slope angle as the direction of camera can be adjusted accordingly. Such an optimal orientation is lost when mapping a highly inclined terrain with LIDAR. Table 3 illustrates the decrease in LIDAR mapping accuracy as a function of the steepness of the slope and the homogeneity of the terrain. We conclude that if the accuracy of a laser scanner on a homogenous slope of  $10^\circ$  is satisfying, the errors rise quickly and above the permissible level for the  $40^\circ$  inclined slope. That is also the case on terrain that is mixed with snow and rocks. This assessment was carried out using a 20cm terrain grid obtained by the laser scanner and the independently surveyed control points. The manifested dependence of LIDAR mapping accuracy on the homogeneity of the terrain corresponds well with the values reported by Berg and Ferguson, 2001.

Method	Homogenous Terrain	Mixed Terrain
	$10^\circ$	$40^\circ$
LIDAR, GPS/INS	17cm	30cm
Handheld Camera, GPS/INS	$\leq 20\text{cm}$ in all cases	

Table 3. Comparison between the mapping accuracy of a LIDAR and the developed system on different terrain.

## 6. CONCLUSIONS

The developed handheld mapping system for natural hazard mapping is now operational and following conclusions can be drawn with respect to its characteristics:

- The system can be quickly deployed into inaccessible areas as its concept is independent of a carrier.
- Use of GPS/INS onboard provides an adequate accuracy in the object space without any ground control or tie points.
- The terrain is mapped with a consistent accuracy of  $\leq 20$ cm regardless of steepness and character.

Waypoint Consulting Inc., 2001. GrafNav/GrafMov Operating Manual v603a, Suite 210, 200 Rivercrest Drive S.E., Calgary, Alberta T2C 2X5, August 2001, <http://www.waypnt.com>.

When compared to LIDAR, the constructed system seems to be better suited for small mapping tasks in mountainous regions in terms of accuracy, flexibility and cost.

### ACKNOWLEDGMENTS

Flight time and expertise was supplied by Air Glacier Switzerland. Their support and friendliness is greatly acknowledged. The Tomtecs Corp. is thanked for providing the camera and Altex Corp. for offering their laser scanning services free of charge. Many thanks also belong to Mr. Didier Jacquemettaz for his excellent work in the field and the evaluation of the control data. Finally, we thank Dr. W. Ammann, Dr. V. Gruber and Mr. F. Dufour of the Swiss Federal Institute for Snow and Avalanche Research for their active participation in this research project.

### REFERENCES

Applanix Corp., 2000. POSProc User Manual v2.1, 85 Leek Crescent, Ontario, L4B 3B3, <http://www.applanix.com>.

Berg, R., Ferguson, J. 2001. Mapping Ontario's Highways with Lidar, *GIM International*, Vol. 15, Issue 11, November 2001, pp. 12-15.

DRC, 2001. VME-NAV User Manual (Force 5 version), Dynamic Research Corporation, Test Equipment Division, 93 Border Street, West Newton, MA 02165, April 2001, <http://www.drc.com>.

Kruck, E., 2001. Bingo-F User's Manual, GIP - Gesellschaft für Industriephotogrammetrie mbH, D-73430 Aalen, Germany.

Issler, D., 1999. European Avalanche Test Sites. Overview and Analysis in view of co-ordinated experiments. *Mitteilungen* #59, 1999. SLF Davos.

Skaloud, J., 2002. Direct Georeferencing in Aerial Photogrammetric Mapping, PE&RS, *Journal of Photogrammetric Engineering & Remote Sensing*, March 2002, pp. 207-210.

Schmitz, M., Wübbena, G., Bagge, A., 2001. Benefit of Rigorous Modeling of GPS in Combined AT/GPS/IMU-Bundle Block Adjustment, OEEPE-Workshop on Integrated Sensor Orientation, Hannover, Germany, Hannover, Germany.

Vallet, J., Skaloud, J., Koelbl, O., Merminod, B., 2000. Development of a Helicopter-Based Integrated System for Avalanche Mapping and Hazard Management, *The International Archives of the Photogrammetry, Remote Sensing and Spatial Information Sciences*, Amsterdam, Vol. XXXIII, Part B2, pp. 565-572